Am J Cancer Res 2024;14(4):1904-1913
www.ajcr.us /ISSN:2156-6976/ajcr0155584

*Original Article*

# Screening and identification of serum exosomal protein ZNF587B in liquid biopsy for ovarian cancer diagnosis

Hu Li[1*], Tiantian Sui[1*], Xiaoxiao Chen[1*], Yanqiong Gu[1], Xuezhen Luo[2], Yiyao Liu[1], Qizhi He[1]

*[1]Department of Pathology, Shanghai First Maternity and Infant Hospital, School of Medicine, Tongji University, Shanghai 201204, China; [2]Department of Gynecology, Obstetrics and Gynecology Hospital of Fudan University, Shanghai 200011, China. [*]Equal contributors.*

Received January 23, 2024; Accepted March 31, 2024; Epub April 15, 2024; Published April 30, 2024

**Abstract:** Addressing the critical challenge of early ovarian cancer (OC) detection, our study focuses on identifying novel biomarkers by analyzing preoperative peripheral blood exosomes from high-grade serous ovarian cancer (HGSC) patients and healthy controls. Utilizing high-performance liquid chromatography-mass spectrometry-based quantitative proteomics, we isolated and analyzed peripheral blood exosomes to identify differentially expressed proteins (DEPs). This comprehensive analysis, supported by gene ontology enrichment and Kyoto Encyclopedia of Genes and Genomes (KEGG) database assessments, revealed 28 proteins with decreased abundance and 33 with increased abundance in HGSC patients compared to controls. Notably, Zinc Finger Protein 587B (ZNF587B) exhibited a significant reduction in abundance, confirmed by decreased mRNA and protein levels in HGSC and normal ovarian tissues, consistent with omes exosomal protein expression levels. Immunohistochemical staining further confirmed reduced ZNF587B protein levels in HGSC tissues. The significant correlation between ZNF587B expression levels and tumor stage underscores its potential as a valuable biomarker for early liquid biopsy screening of OC. Our findings suggest ZNF587B plays a crucial role in early HGSC detection, highlighting the importance of further research to validate its clinical utility and improve ovarian cancer patient outcomes.

**Keywords:** Ovarian cancer, ZNF587B, liquid biopsy, exosomes

## Introduction

Ovarian cancer (OC) bears the highest mortality rate among gynecological malignancies [1]. At the time of diagnosis, 60-70% of patients present at an advanced stage, with a 5-year survival rate ranging between 20-30% [2]. Currently, clinical diagnosis and screening primarily rely on a combination of the serum tumor marker CA125 and transvaginal ultrasound. However, the sensitivity and specificity of these methods remain unsatisfactory [3]. Therefore, there is an urgent need to identify sensitive and specific methods for early diagnosis and screening of OC, to reduce mortality rates and improve the 5-year survival rate [4].

Pathological diagnosis remains the gold standard for OC diagnosis [5]. Traditional histology, imaging techniques, and related serum tumor markers play pivotal roles in clinical diagnosis [6]. Nevertheless, with ongoing advancements in bioinformatics and molecular biology, there is a deeper comprehension of the molecular mechanisms underlying tumor initiation and progression [7, 8]. The limitations of traditional diagnostic approaches, such as inherent subjectivity, are increasingly evident, posing challenges in providing a comprehensive and accurate reflection of tumor characteristics [9]. Hence, we have developed a novel liquid biopsy method. Compared to traditional tissue biopsy, liquid biopsy offers numerous advantages, including rapidity, convenience, and minimal invasiveness [10, 11], thus holding significant application potential in clinical settings [12, 13]. In liquid biopsy, tumors or other diseases are diagnosed by detecting bioactive molecules in bodily fluids such as blood or urine [14]. One of its primary advantages lies in noninvasive sampling. Additionally, it demonstrates high sensitivity and fast detection, facilitating early tumor detection [15]. Liquid biopsy targets three categories of bioactive molecules: free DNA, circulating tumor cells, and exosomes. Levels of free DNA and circulating tumor cells in the blood-

stream are exceedingly low [16], with as few as 1-10 tumor cells per milliliter of circulating blood, making their enrichment challenging. Conversely, bioactive exosomes released by tumor cells are abundant in bodily fluids (exceeding $10^9$/ml of blood), rendering the detection of exosomes highly sensitive, thereby aiding in early tumor diagnosis [17]. Moreover, the lipid bilayer membrane structure of exosomes confers robust protection, shielding exosome contents from degradation by blood circulation enzymes, thereby enhancing stability [18]. Due to their small size, exosomes possess strong tissue barrier penetration capabilities, facilitating easy access to various bodily fluids, a crucial prerequisite for liquid biopsy [16, 19].

Exosomes are vesicles formed within endosomes and are gradually released from the cell through budding. They typically have diameters of less than 100 nm [20]. Comprising a variety of bioactive substances such as microRNAs, long non-coding RNA, circular RNA, and proteins, exosomes play diverse biological roles [21]. Extracellular vesicles were isolated from the peripheral blood of five patients with high-grade serous ovarian cancer (HGSC) and five healthy volunteers via ultracentrifugation. Their morphology was observed using transmission electron microscopy, and the presence of the markers CD9 and CD81 was confirmed through western blotting, validating their identity as exosomes. Exosome proteomics was analyzed using high-performance liquid chromatography-mass spectrometry (HPLC-MS), identifying 267 proteins, with 61 showing a 1.2-fold increase in abundance. Differentially expressed proteins (DEPs) were categorized based on secondary functions using gene ontology (GO) and analyzed through the Kyoto Encyclopedia of Genes and Genomes (KEGG) pathway database. As a result, ZNF587B was identified as potential research target. Notably, there are no existing studies on the role of this protein in exosomes and ovarian cancer, and it exhibits the largest deviation from the conventional classification and quantification categories in the test results.

## Materials and methods

### *Patients and tissue samples*

A total of 10 plasma samples were collected between 2017 and 2018 from the Shanghai First Maternity and Infant Hospital (Shanghai, China). This included 5 plasma samples from patients diagnosed with high-grade serous ovarian cancer (HGSC) and 5 samples from healthy individuals. Diagnosis of HGSC in patients was confirmed through histological examination of tissue biopsy, and none had received radiotherapy, endocrine therapy, chemotherapy, or surgery before blood sample collection. Written informed consent was obtained from all participants, including patients and healthy individuals. This study was approved by the Ethics Committee of the Shanghai First Maternity and Infant Hospital (approval number: KS18112).

### *Extraction and identification of exosomes from peripheral blood*

Whole-blood samples were collected in ethylenediaminetetraacetic acid (EDTA)-coated plasma tubes to prevent coagulation. The collection was conducted under standardized conditions to minimize cellular perturbations and ensure exosome integrity. Upon collection, samples were promptly centrifuged at 1,600×g for 15 minutes at room temperature to separate the plasma. The plasma layer was carefully aspirated without disturbing the buffy coat and transferred to polypropylene tubes, known for their low protein-binding properties, thus preserving the native state of the exosomes. These samples were then maintained at 2-8°C and processed within 2 hours of collection to isolate exosomes, ensuring minimal degradation and maintaining sample fidelity for subsequent proteomic analysis. Serum exosomes were extracted using ExoQuick exosome precipitation solution (Cat. No. EXOQ5A-1). Plasma was collected by centrifuging at 3000×g for 15 minutes to remove cells or cell fragments. The supernatant was transferred to a clean sterilization tube, and ExoQuick reagent was added. The mixture was incubated at 37°C for 15 minutes and then centrifuged again at 10,000×g for 5 minutes at 25°C. The supernatant was transferred to another clean sterilization tube, and the pellet was discarded. Next, 25 µl of ExoQuick reagent was added to every 100 µl of supernatant and mixed evenly, followed by overnight incubation at 4°C (or at least 12 hours). After centrifugation at 1500×g for 30 minutes at room temperature or 4°C, the supernatant was removed, centrifuged again at 1500×g for 5 minutes, and the liquid compo-

nents in the upper layer were carefully removed. Then, 1/10 of the original volume of sterile water or nuclease-free water was added to resuspend the precipitate until completely dissolved. Protein quantification was performed using the bicinchoninic acid (BCA) assay.

*Proteomic analysis of exosomes by HPLC-MS*

The peptides were fractionated using high-pH reversed-phase HPLC, employing an Agilent 300 Extend C18 column (5 μm particle size, 4.6 mm inner diameter, 250 mm length). The peptide fractionation gradient consisted of 8-32% acetonitrile at pH 9, separating 60 fractions over 60 minutes, which were then combined into nine fractions and subsequently freeze-dried for further analysis.

The peptides were reconstituted in an LC mobile phase containing 0.1% (v/v) aqueous formic acid and separated using an Easy-nLC 1000 ultra-high-performance liquid chromatography system. Mobile phase A consisted of 0.1% formic acid in 2% acetonitrile, while mobile phase B comprised 0.1% formic acid in 90% acetonitrile. The liquid chromatography gradient settings were as follows: 0-26 min, 9-25% B; 26-34 min, 25-36% B; 34-37 min, 36-80% B; 37-40 min, 80% B; with a flow rate of 700 nL/min. Following chromatographic separation, peptides were introduced into a nanospray ionization (NSI) source and analyzed by an Orbitrap Fusion™ mass spectrometer. The ion source voltage was set at 2.0 kV, and both the parent ions and their fragments were detected and analyzed by high-resolution Orbitrap. The primary mass spectrometer scanned a range of 350-1550 m/z at a resolution of 60,000, while the secondary MS scanned a fixed range of 100 m/z at a resolution of 15,000. Data were acquired using a data-dependent scanning (DDA) program, where the top 20 peptide segments with the highest signal intensity were selected for Higher-energy C-trap dissociation (HCD) collision-induced fragmentation. To enhance MS efficiency, the automatic gain control was set to 5e4, the signal threshold to 5000 ions/s, the maximum injection time to 200 ms, and a dynamic exclusion time of 30 s was applied to prevent repetitive scanning of parent ions.

*RNA isolation and real-time PCR*

Total RNA was extracted using the TRIzol reagent (Invitrogen, Carlsbad, CA, USA) following the manufacturer's protocol, and reverse transcription was carried out using a PrimeScript RT Reagent Kit (TaKaRa, Shanghai, China). RNA concentration and purity were assessed using an Agilent Technologies 2100 Bioanalyzer. Quantitative real-time polymerase chain reaction (qRT-PCR) experiments were conducted using 7500 Real-Time PCR Systems (Applied Biosystems). Analyses were performed in triplicate for each sample using the SYBR Green PCR Kit (Applied Biosystems, Waltham, MA, USA) over 40 cycles. The qRT-PCR cycling protocol included a 3-step thermal cycling sequence: initial denaturation at 94°C for 15 seconds, annealing at 55°C for 30 seconds, followed by extension at 70°C for 30 seconds. To ensure amplification specificity, a melting curve analysis was conducted post-amplification. The primer sequences used for qRT-PCR are detailed as follows: ZNF587B-F, 5'-CAGTGGACGACTTCATGGCT-3'; and ZNF587B-R, 5'-CCTCAACAGTACCGAGCACA-3'. The expression levels from qRT-PCR were calculated using the $2^{-\Delta\Delta Ct}$ method.

*Western blotting*

Proteins were extracted from tissue lysates and lysed in Tissue Protein Extraction Reagent (Thermo Scientific, MA, USA) supplemented with a 1× phosphatase inhibitor cocktail and 1× protease inhibitor cocktail (Roche) for 5 minutes on ice, followed by centrifugation (12,000 rpm, 4°C, 15 minutes). Soluble proteins in the supernatant were separated by sodium dodecyl sulfate-polyacrylamide gel electrophoresis (SDS-PAGE) and transferred onto nitrocellulose membranes (Bio-Rad, Hercules, CA, USA). Nonspecific binding was blocked by incubating the membranes in 5% non-fat milk for 1 hour at room temperature. Subsequently, the membranes were incubated overnight at 4°C with either an anti-ZNF587B monoclonal antibody (1:1000; Affinity Company customization) or an anti-CD81 polyclonal antibody. After washing with phosphate-buffered saline containing 1% Tween 20 (PBST), the membranes were incubated with horseradish peroxidase (HRP)-conjugated anti-mouse or anti-rabbit secondary antibodies (1:2000, Jackson) at room temperature for 2 hours and then washed again with PBST. Western blots were visualized using an enhanced chemiluminescence (ECL) detection reagent and an ECL kit (Thermo Scientific). A monoclonal anti-GAPDH-peroxidase antibody (1:2500, ab9485, Abcam) se-

**Table 1.** Clinicopathological information in 5 HGSC patients

| ID | Age | FIGO | Tumor grade | ER | PR | Ki-67 |
|---|---|---|---|---|---|---|
| Sample01 | 63 | $IC_1$ | G3 | + | - | 70%+ |
| Sample02 | 54 | IA | G3 | + | + | 40%+ |
| Sample03 | 59 | IA | G3 | + | - | 60%+ |
| Sample04 | 50 | IB | G3 | - | - | 50%+ |
| Sample05 | 49 | IA | G3 | + | - | 80%+ |

rved as an internal loading control to assess the amount of loaded protein.

*Immunohistochemistry (IHC)*

Human primary HGSC tissue sections were probed with a monoclonal antibody against ZNF587B (1:100; customized by Affinity Company), followed by the application of an HRP-conjugated secondary antibody. Preparation of the HGSC tissue microarray and IHC procedures were conducted following previously described protocols [22].

*Statistical analysis*

Sample size determination for this study was based on a preliminary analysis aimed at ensuring adequate statistical power to detect significant differences in the primary outcomes of interest, while also considering ethical implications by utilizing the minimum necessary samples. Based on these considerations, a minimum of five samples per group was deemed necessary. This approach is consistent with recommendations from similar studies and was validated by consulting with a statistician specializing in biomedical research.

Statistical analysis was performed using SPSS 13.0 software, and data are presented as mean ± standard deviation. Differences between the two groups were analyzed using Student's t-test, with statistical significance set at $P < 0.05$.

## Results

*Identification of exosomes in HGSC peripheral blood*

Exosomes were isolated from the peripheral blood of five patients with HGSC and five healthy volunteers using ultracentrifugation. The demographic information and clinical characteristics of the five patients are detailed in **Table 1**. Transmission electron microscopy was employed to observe the morphology. Additionally, western blotting was conducted to detect exosome markers, confirming the identity of the extracted extracellular vesicles as exosomes.

Transmission electron microscopy analysis revealed that exosomes from both healthy volunteers and patients with HGSC exhibited a classic cup-shaped bilayer membrane structure, with diameters ranging from 10 to 100 nm (**Figure 1A**). The exosome membrane displayed enrichment of transmembrane proteins involved in exosome transport, including CD63, CD81, and CD9, as well as heat shock proteins (HSP60, HSP70, and HSPA5). Western blotting confirmed the presence of transmembrane proteins CD63, CD81, and HSP70 in the samples (**Figure 1B**). Nanoparticle tracking analysis demonstrated that the average diameter of exosomes in both the experimental and control groups fell within the range of 40-100 nm (**Figure 1C**). Furthermore, the analysis revealed that the exosome protein concentration in the experimental group was comparable to that in the control group (**Figure 1D**).

*Differential expression of exosome proteins in HGSC peripheral blood*

The proteomics analysis of exosomes isolated from peripheral blood was conducted using HPLC-MS, revealing the identification of 267 proteins, among which 61 proteins exhibited a 1.2-fold increase in abundance. These DEPs were further categorized based on their secondary functions according to the GO classification and analyzed utilizing the KEGG pathway (**Figure 2A-F**). In comparison with the control group, the experimental group displayed 28 proteins with decreased abundance and 33 proteins with increased abundance. The 61 identified proteins were classified into four categories, designated as Q1-Q4, based on the conventional classification and quantitative assessment of the C/D ratio (**Table 2** and **Figure 2E**). Exploring databases such as the OC Serum Marker Database, Clinical Proteomics Data Bank, Proteomics Identification Database, and Proteomics DB, we observed minimal research on the ZNF587B protein in the context of OC. Notably, the expression abun-

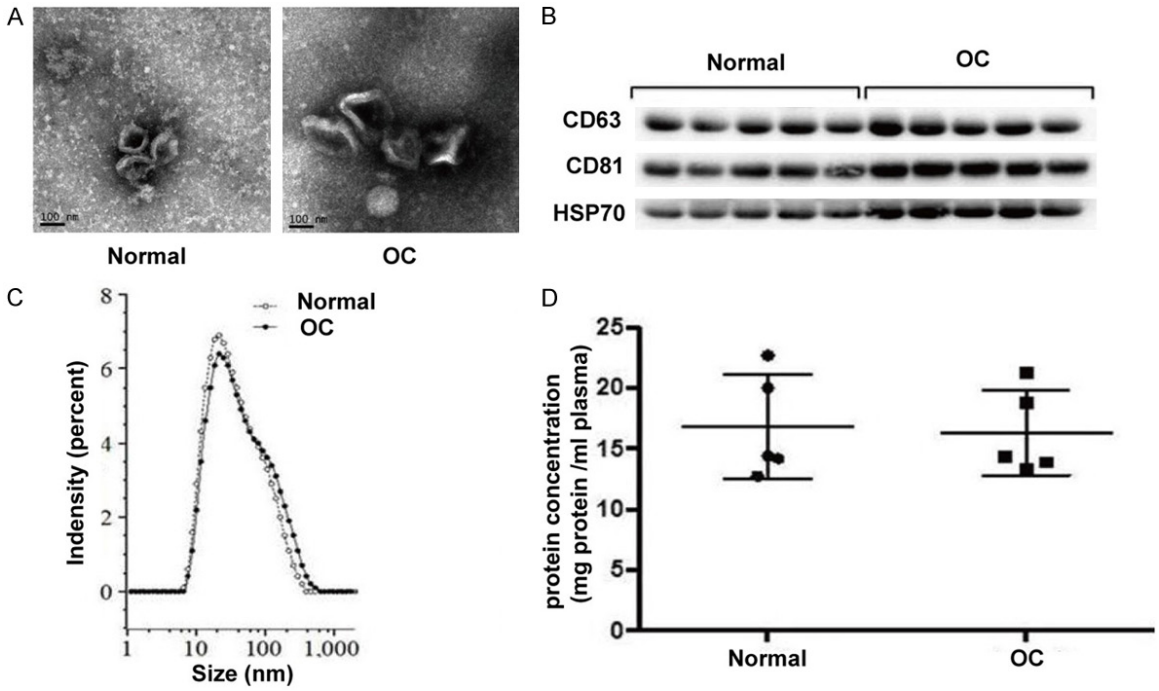


**Figure 1.** Identification of exosomes in HGSC peripheral blood. A. Transmission electron microscopy shows the classic cup-shaped bilayer membrane structure (100 nm) of exosomes from both normal individuals and HGSC patients; B. Western blot confirms the presence of transmembrane proteins CD63, CD81, and heat shock protein HSP70 in our samples; C. Nanoparticle tracking analysis reveals the average diameter distribution of exosomes in the experimental and control groups to be 40-100 nm; D. Exosomal protein concentration in the experimental group is comparable to that of the control group.

dance of ZNF587B protein was found to be low in peripheral blood serum, and it has not been previously reported as a serum marker for OC. Therefore, we postulated that this protein might be specific to exosomes and could potentially serve as a diagnostic marker for liquid biopsy in exosomes. Thus, based on our preliminary findings, we aim to further validate its utility and reliability.

*Expression of ZNF587B was decreased abundance in HGSC tissue*

We assessed ZNF587B expression in primary HGSC tissues (T) and compared it with the expression in corresponding normal ovarian tissues (N) using western blot analysis (**Figure 3A**). ZNF587B protein expression was found to be decreased in HGSC tissues. Additionally, we detected the endogenous expression of ZNF587B mRNA in HGSC patient tissues and matched normal ovarian tissues using real-time PCR, revealing a significant decrease in ZNF587B mRNA expression in HGSC compared to the control group (**Figure 3B**). These findings were further confirmed by analyzing the protein expression of ZNF587B in 59 normal ovarian tissues (**Figure 3C**) and 59 primary HGSC tissues (**Figure 3D**) using immunohistochemistry (IHC). The IHC results were categorized into two groups: high ZNF587B expression (score of 3 or 4) and low ZNF587B expression (weak or no staining, score of 0, 1, or 2). Our analysis revealed that 84.7% of normal ovarian tissues (50/59) displayed high positive staining, whereas 79% of HGSC tissues (47/59) showed low staining. Thus, the observed downregulation of ZNF587B in HGSC tissues prompted further exploration of its clinical significance.

*Low expression of ZNF587B is correlated with poor prognosis in HGSC*

Low expression of ZNF587B correlates with poor prognosis in HGSC. Our previous studies have demonstrated a common reduction of ZNF587B levels in HGSC compared to adjacent normal tissues. Utilizing data from TCGA, Kaplan-Meier survival analysis revealed that diminished ZNF587B expression was associat-

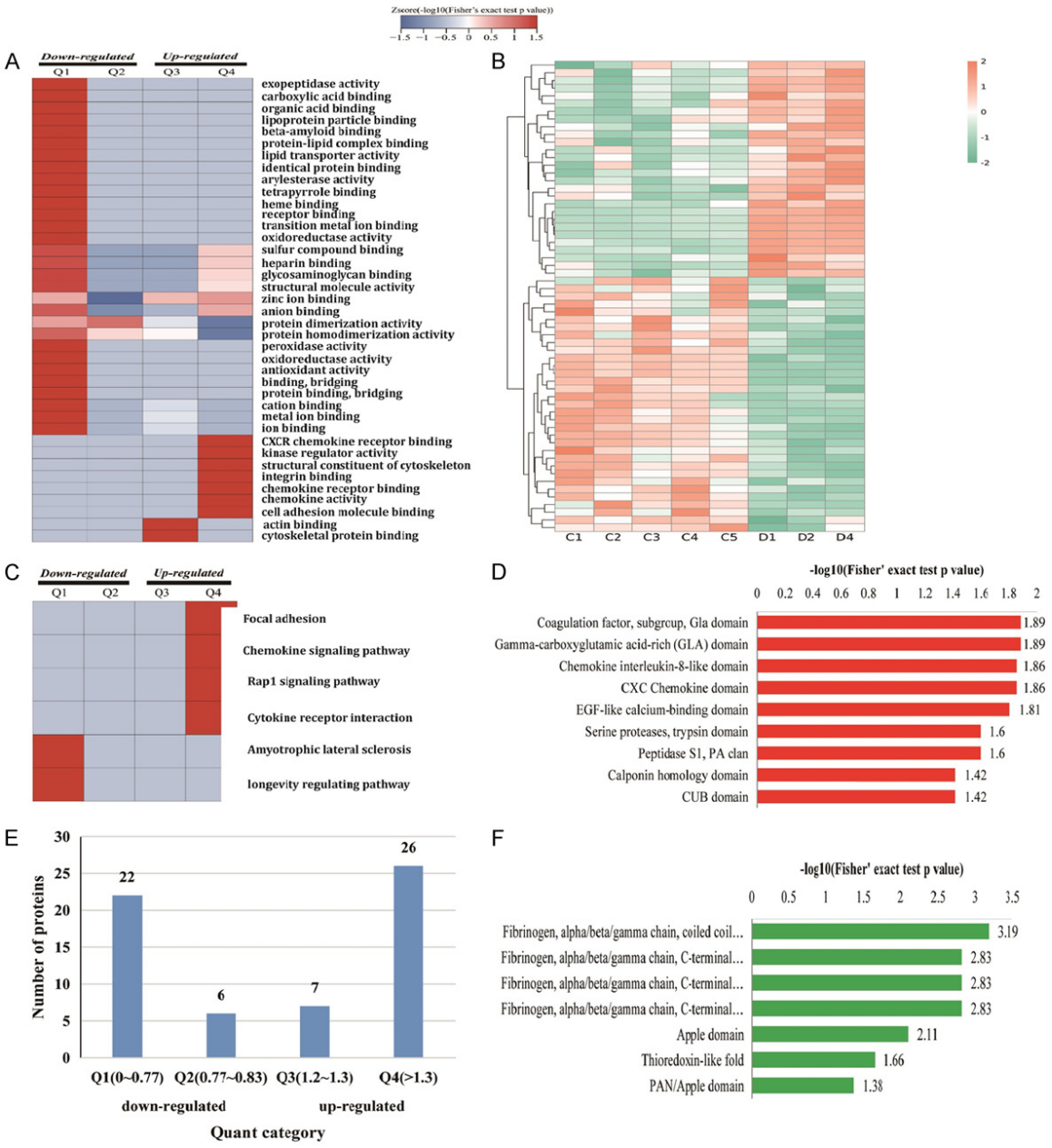


**Figure 2.** Differential expression of exosomal proteins in peripheral blood. (A) Heat map of exosomal protein molecular function based on gene ontology enrichment cluster analysis; (B) Differential expression of proteins (DEPs) categorized by their fold changes; (C) Functional analysis of exosomal protein domains based on KEGG pathway enrichment; (D) Protein domain enrichment map of upregulated proteins and (F) downregulated proteins; (E) DEPs categorized into four groups based on their fold changes, designated as Q1 to Q4. Q1 (0 < ratio ≤ 1/1.3 and P < 0.05), Q2 (1/1.3 < ratio ≤ 1/1.2 and P < 0.05), Q3 (1.2 < ratio ≤ 1.3 and P < 0.05), and Q4 (ratio > 1.3 and P < 0.05).

**Table 2.** Differential expression of exosome proteins

| Regulation | Quant category | Number of proteins |
|---|---|---|
| Decreased abundance | Q1 (0-0.77) | 22 |
| | Q2 (0.77-0.83) | 6 |
| Increased abundance | Q3 (1.2-1.3) | 7 |
| | Q4 (> 1.3) | 26 |

ed with shorter OS times (P = 0.009), indicating that reduced ZNF587B expression may contribute to unfavorable prognosis in HGSC (**Figure 4A**). Importantly, TCGA data analysis did not reveal a direct correlation between ZNF587B expression and tumor grade (**Figure 4B**). Comparative analysis confirmed that ZNF587B expression levels in HGSC patients were significantly lower than those in individuals with-

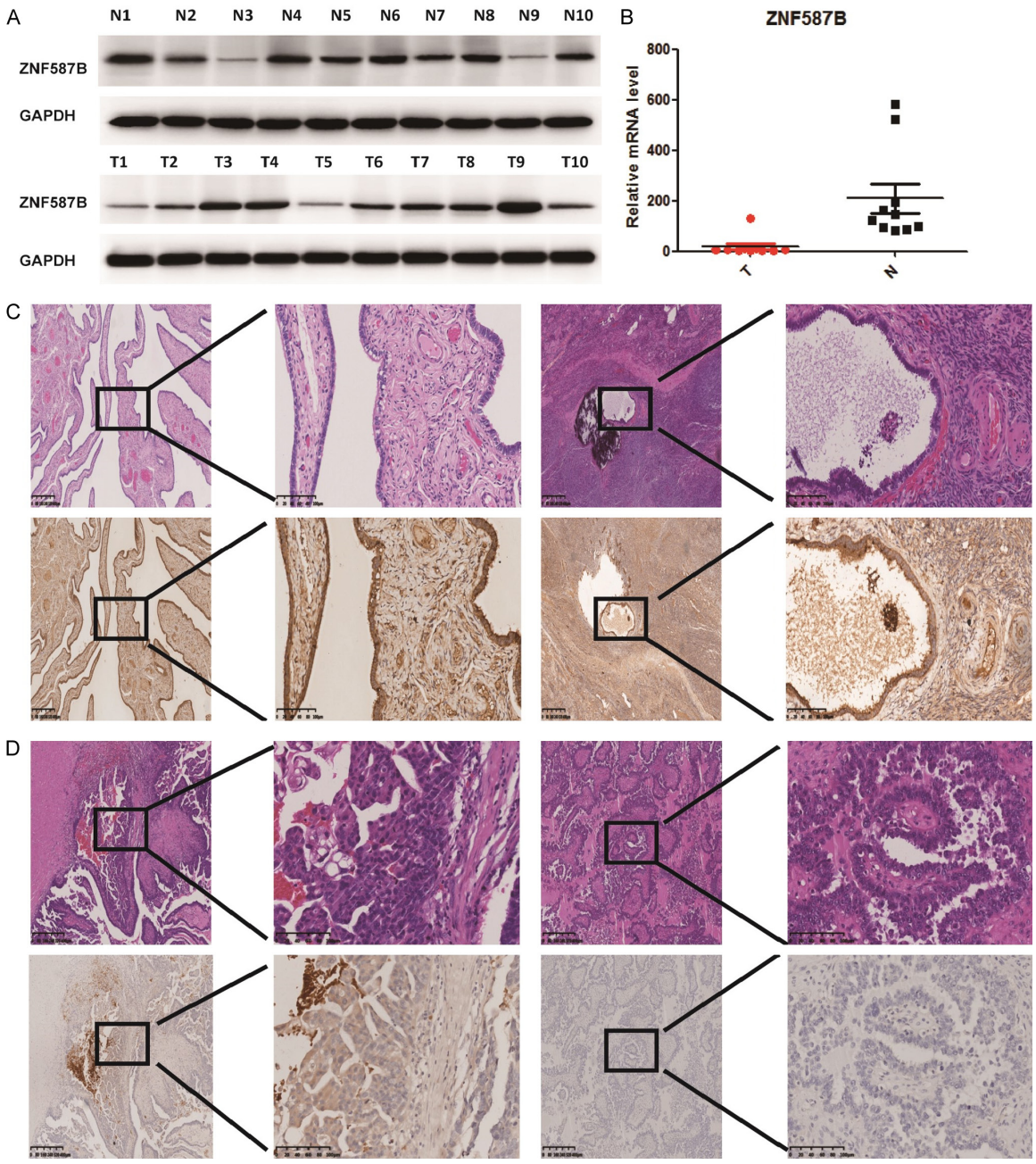


**Figure 3.** Decreased expression of ZNF587B in HGSC tissues. A. Western blot analysis of ZNF587B expression in primary HGSC patient tissues (T) compared with matched normal ovarian tissues (N); B. Real-Time PCR showing endogenous expression of ZNF587B mRNA in HGSC patient tissues and matched normal ovarian tissues; C. Analysis of ZNF587B protein expression in 59 normal ovarian tissues; D. Immunohistochemistry demonstrating high positive staining in (50/59) 84.7% of normal ovarian tissues and low staining in HGSC tissues (47/59) 79%.

out cancer, underscoring the importance of ZNF587B as a biomarker (**Figure 4C**). This evidence, based on TCGA data, firmly establishes the clinical relevance of ZNF587B expression in HGSC and provides a valuable prognostic marker.

## Discussion

*ZNF587B* is a novel cisplatin-sensitive gene identified in our previous study through HPLC-MS analysis of exosomes from the peripheral blood of patients with HGSC [23]. ZNF587B

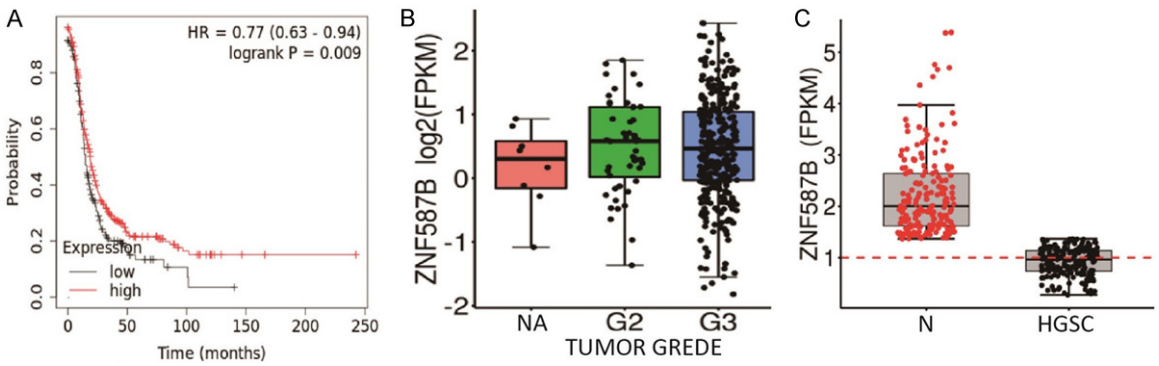


**Figure 4.** Low expression of ZNF587B correlates with poor prognosis in HGSC. A. Kaplan-Meier survival analysis reveals that lower ZNF587B levels are associated with shorter overall survival (OS) time (P = 0.009), suggesting a potential role of low ZNF587B expression in poor HGSC prognosis; B. No correlation is found between ZNF587B expression and tumor grade; C. ZNF587B expression level in HGSC is significantly lower than in normal individuals (P < 0.05). Abbreviations: HR: Hazard Ratio; NA: Not Available; N: Normal.

belongs to the C2H2-type zinc finger protein (ZFP) family [24]. Diseases associated with ZNF587B include transient myeloproliferative syndrome, and many ZFP proteins have been shown to inhibit tumor development and malignancy [25]. However, the function of ZNF587B remains unknown, and its protein has been rarely studied in ovarian carcinoma [26].

HPLC-MS-based quantitative proteomic analysis revealed that ZNF587B expression was 3.292-fold lower in the experimental group compared to the control group. Real-time PCR and western blotting were employed to assess mRNA and protein levels in 10 HGSC and 10 normal ovarian samples. The results demonstrated a decrease in both ZNF587B mRNA and protein levels. Interestingly, this contrasts with the observed protein expression levels in exosomes. Additionally, immunohistochemistry staining indicated a reduced abundance of ZNF587B protein in HGSC compared to normal ovarian tissue. Further analysis, considering patient age, body mass index (BMI), metastasis, chemotherapy history, estrogen receptor (ER) and progesterone receptor (PR) status, clinical tumor grade, pathological tissue type, and other clinical parameters, revealed a significant correlation between ZNF587B expression and tumor stage.

We propose that the ZNF587B protein may be exclusive to exosomes and could serve as a potential marker for liquid biopsy diagnosis of HGSC. Thus, based on preliminary results, further validation of its practicality and reliability is warranted.

Acknowledging the critical limitations of liquid biopsy for ovarian cancer diagnosis, we recognize that significant challenges persist. The sensitivity and specificity of liquid biopsy techniques fluctuate, especially in detecting early-stage ovarian cancer. Tumor heterogeneity and the potential dilution of cancer-specific markers in the bloodstream present substantial obstacles to achieving precise diagnoses. Additionally, the absence of standardized protocols for sample collection, processing, and analysis further amplifies result variability, affecting the reliability and reproducibility of the technique.

Moreover, despite the noninvasive appeal of liquid biopsies, economic and logistical barriers hinder their widespread adoption. The costs associated with testing and the need for specialized equipment and expertise limit accessibility, especially in resource-constrained settings. These challenges highlight the necessity for ongoing research to refine liquid biopsy methodologies, develop standardized protocols, and discover more sensitive and specific biomarkers. Addressing these issues is crucial to enhancing the clinical utility of liquid biopsies in ovarian cancer management.

The advent of precision medicine has allowed for the meticulous treatment of tumors [27]. Traditional morphological and pathological diagnoses cannot keep up with the development of medical treatments [28]. Thus, our study was based on the fact that exosomes are small vesicles with a lipid bilayer membrane structure secreted by cells to protect their genetic

information from tumors. Unlike the need for a large amount of fresh blood in the study of circulating tumor cells, which can detect and reflect the basic characteristics of OC, noninvasive liquid biopsy is a more reliable screening tool in OC [20, 29] to identify potential markers of secreted protein liquid biopsy diagnosis, lay the foundation for early diagnosis and screening of OC, and provide practical methods and tools for reducing ovarian mortality [30].

We investigated the potential of ZNF587B as a biomarker for liquid biopsy in diagnosing ovarian cancer. Our findings suggest that ZNF587B holds significant promise for improving early detection rates. Given the typically late presentation of ovarian cancer symptoms, identifying reliable biomarkers such as ZNF587B is critical for shifting diagnosis to earlier disease stages. Early detection is closely linked to improved patient outcomes, facilitating the timely initiation of treatment strategies that can significantly enhance patient survival rates and quality of life. Furthermore, the noninvasive nature of liquid biopsy offers a patient-friendly alternative to traditional diagnostic methods, potentially increasing patient compliance with screening programs.

However, our study has some limitations. First, the sample size was relatively small, potentially affecting the generalizability of our findings. Additionally, although we demonstrated the diagnostic potential of ZNF587B in ovarian cancer, the specificity and sensitivity of ZNF587B as a stand-alone biomarker remain to be fully elucidated. These aspects are crucial for the clinical application of any biomarker and warrant further investigation.

Future research should aim to validate our findings in larger and more diverse cohorts to confirm the utility of ZNF587B in early ovarian cancer detection. It is also essential to compare ZNF587B with other emerging biomarkers and existing diagnostic modalities to establish its relative performance and potential additive value. Moreover, studies exploring the biological function of ZNF587B in ovarian cancer may provide insights into its role in tumorigenesis and offer new avenues for therapeutic interventions. Finally, integrating ZNF587B into multi-biomarker panels should be considered, as this approach may enhance the diagnostic accuracy and predictive value of liquid biopsies for ovarian cancer.

## Acknowledgements

We thank Dr. Bin Qiao for editing the manuscript.

## Disclosure of conflict of interest

None.

**Address correspondence to:** Drs. Yiyao Liu and Qizhi He, Department of Pathology, Shanghai First Maternity and Infant Hospital, School of Medicine, Tongji University, 2699 West Gaoke Road, Shanghai 201204, China. Tel: +86-21-20261141; E-mail: liuyiyao91@163.com (YYL); qizhihe2013@163.com (QZH)

## References

[1] Nobbenhuis MA, Bancroft E, Moskovic E, Lennard F, Pharoah P, Jacobs I, Ward A, Barton DP, Ind TE, Shepherd JH, Bridges JE, Gore M, Haracopos C, Shanley S, Ardern-Jones A, Thomas S and Eeles R. Screening for ovarian cancer in women with varying levels of risk, using annual tests, results in high recall for repeat screening tests. Hered Cancer Clin Pract 2011; 9: 11.

[2] Alegría-Baños JA, Jiménez-López JC, Vergara-Castañeda A, de León DFC, Mohar-Betancourt A, Pérez-Montiel D, Sánchez-Domínguez G, García-Villarejo M, Olivares-Pérez C, Hernández-Constantino Á, González-Santiago A, Clara-Altamirano M, Arela-Quispe L and Prada-Ortega D. Kinetics of HE4 and CA125 as prognosis biomarkers during neoadjuvant chemotherapy in advanced epithelial ovarian cancer. J Ovarian Res 2021; 14: 96.

[3] Cheng X, Zhang L, Chen Y and Qing C. Circulating cell-free DNA and circulating tumor cells, the “liquid biopsies” in ovarian cancer. J Ovarian Res 2017; 10: 75.

[4] Chava S, Bugide S, Edwards YJK and Gupta R. Disruptor of telomeric silencing 1-like promotes ovarian cancer tumor growth by stimulating pro-tumorigenic metabolic pathways and blocking apoptosis. Oncogenesis 2021; 10: 48.

[5] Zhou Q, Li W, Leng B, Zheng W, He Z, Zuo M and Chen A. Circulating cell free DNA as the diagnostic marker for ovarian cancer: a systematic review and meta-analysis. PLoS One 2016; 11: e0155495.

[6] He QZ, Luo XZ, Wang K, Zhou Q, Ao H, Yang Y, Li SX, Li Y, Zhu HT and Duan T. Isolation and characterization of cancer stem cells from high-grade serous ovarian carcinomas. Cell Physiol Biochem 2014; 33: 173-84.

[7] Luo XZ, He QZ and Wang K. Expression of Toll-like receptor 4 in ovarian serous adenocarci-

noma and correlation with clinical stage and pathological grade. Int J Clin Exp Med 2015; 8: 14323-7.
[8] Seborova K, Vaclavikova R, Soucek P, Elsnerova K, Bartakova A, Cernaj P, Bouda J, Rob L, Hruda M and Dvorak P. Association of ABC gene profiles with time to progression and resistance in ovarian cancer revealed by bioinformatics analyses. Cancer Med 2019; 8: 606-616.
[9] Au KK, Josahkian JA, Francis JA, Squire JA and Koti M. Current state of biomarkers in ovarian cancer prognosis. Future Oncol 2015; 11: 3187-95.
[10] Giannopoulou L, Zavridou M, Kasimir-Bauer S and Lianidou ES. Liquid biopsy in ovarian cancer: the potential of circulating miRNAs and exosomes. Transl Res 2019; 205: 77-91.
[11] Imamura T, Komatsu S, Ichikawa D, Kawaguchi T, Miyamae M, Okajima W, Ohashi T, Arita T, Konishi H, Shiozaki A, Morimura R, Ikoma H, Okamoto K and Otsuji E. Liquid biopsy in patients with pancreatic cancer: circulating tumor cells and cell-free nucleic acids. World J Gastroenterol 2016; 22: 5627-41.
[12] Pantel K and Alix-Panabières C. Bone marrow as a reservoir for disseminated tumor cells: a special source for liquid biopsy in cancer patients. Bonekey Rep 2014; 3: 584.
[13] Fenizia F, De Luca A, Pasquale R, Sacco A, Forgione L, Lambiase M, Iannaccone A, Chicchinelli N, Franco R, Rossi A, Morabito A, Rocco G, Piccirillo MC and Normanno N. EGFR mutations in lung cancer: from tissue testing to liquid biopsy. Future Oncol 2015; 11: 1611-23.
[14] Zhu Y, Yang T, Wu Q, Yang X, Hao J, Deng X, Yang S, Gu C and Wang Z. Diagnostic performance of various liquid biopsy methods in detecting colorectal cancer: a meta-analysis. Cancer Med 2020; 9: 5699-5707.
[15] Heitzer E, Ulz P and Geigl JB. Circulating tumor DNA as a liquid biopsy for cancer. Clin Chem 2015; 61: 112-23.
[16] Li X and Wang X. The emerging roles and therapeutic potential of exosomes in epithelial ovarian cancer. Mol Cancer 2017; 16: 92.
[17] Minciacchi VR, Freeman MR and Di Vizio D. Extracellular vesicles in cancer: exosomes, microvesicles and the emerging role of large oncosomes. Semin Cell Dev Biol 2015; 40: 41-51.
[18] Zhang W, Peng P, Kuang Y, Yang J, Cao D, You Y and Shen K. Characterization of exosomes derived from ovarian cancer cells and normal ovarian epithelial cells by nanoparticle tracking analysis. Tumour Biol 2016; 37: 4213-21.
[19] Kim Y, Jeon J, Mejia S, Yao CQ, Ignatchenko V, Nyalwidhe JO, Gramolini AO, Lance RS, Troyer DA, Drake RR, Boutros PC, Semmes OJ and Kislinger T. Targeted proteomics identifies liquid-biopsy signatures for extracapsular prostate cancer. Nat Commun 2016; 7: 11906.
[20] Dorayappan KDP, Wallbillich JJ, Cohn DE and Selvendiran K. The biological significance and clinical applications of exosomes in ovarian cancer. Gynecol Oncol 2016; 142: 199-205.
[21] Shen X, Wang C, Zhu H, Wang Y, Wang X, Cheng X, Ge W and Lu W. Exosome-mediated transfer of CD44 from high-metastatic ovarian cancer cells promotes migration and invasion of low-metastatic ovarian cancer cells. J Ovarian Res 2021; 14: 38.
[22] Liu YY, Wang QP, Liu FF, Zhu HT and He QZ. Comparative study of BRAF gene mutations in ovarian serous tumors by immunohistochemistry and DNA sequencing. J BUON 2021; 26: 670-676.
[23] Ouyang Q, Liu Y, Tan J, Li J, Yang D, Zeng F, Huang W, Kong Y, Liu Z, Zhou H and Liu Y. Loss of ZNF587B and SULF1 contributed to cisplatin resistance in ovarian cancer cell lines based on Genome-scale CRISPR/Cas9 screening. Am J Cancer Res 2019; 9: 988-998.
[24] Liu Y, Ouyang Q, Sun Z, Tan J, Huang W, Liu J, Liu Z, Zhou H, Zeng F and Liu Y. The novel zinc finger protein 587B gene, ZNF587B, regulates cell proliferation and metastasis in ovarian cancer cells in vivo and in vitro. Cancer Manag Res 2020; 12: 5119-5130.
[25] Lee SH, Kim HP, Kang JK, Song SH, Han SW and Kim TY. Identification of diverse adenosine-to-inosine RNA editing subtypes in colorectal cancer. Cancer Res Treat 2017; 49: 1077-1087.
[26] Pelleri MC, Piovesan A, Caracausi M, Berardi AC, Vitale L and Strippoli P. Integrated differential transcriptome maps of Acute Megakaryoblastic Leukemia (AMKL) in children with or without Down Syndrome (DS). BMC Med Genomics 2014; 7: 63.
[27] Rajagopal C and Harikumar KB. The origin and functions of exosomes in cancer. Front Oncol 2018; 8: 66.
[28] Yu J, Huang Y, Lin C, Li X, Fang X, Zhong C, Yuan Y and Zheng S. Identification of kininogen 1 as a serum protein marker of colorectal adenoma in patients with a family history of colorectal cancer. J Cancer 2018; 9: 540-547.
[29] Cai J, Gong L, Li G, Guo J, Yi X and Wang Z. Exosomes in ovarian cancer ascites promote epithelial-mesenchymal transition of ovarian cancer cells by delivery of miR-6780b-5p. Cell Death Dis 2021; 12: 210.
[30] Yang C, Kim HS, Song G and Lim W. The potential role of exosomes derived from ovarian cancer cells for diagnostic and therapeutic approaches. J Cell Physiol 2019; 234: 21493-21503.